# Land Cover Mapping: A Comparative Study of Deeplabv3+ and Tiramisu on LISS-III Data

Nirav Desai 1*[0000-0002-5385-9674],
Akruti Naik 1[0000-0003-1006-8693]
1 D-UIAS AND D-SIM&C,Valsad, INDIA
*Corresponding author's : niravdesai.research@gmail.com
akrutinaikdesai@gmail.com

## Abstract:

Assessing land utilization and coverage, along with evaluating cultivated areas across different categories, is an essential endeavor. Traditional approaches for such assessments are typically labor-intensive, time-consuming, and expensive. Remote Sensing (RS) provides a more efficient and cost-effective alternative by delivering distinctive and valuable insights. This study utilized LISS-III (Linear Imaging Self-Scanning Sensor-III) imagery, which records data within specific wavelength ranges of the electromagnetic spectrum (EM), featuring resolutions beyond 100 nm and fewer than 10 spectral bands. To categorize each pixel in the RS images, semantic segmentation was employed, ensuring precise classification. This technique involves pixel-wise categorization, where every pixel is assigned to a designated class. The research identified four distinct classes: water bodies, barren land, residential zones, and vegetative regions. This study utilized DeepLabv3+ and Tiramisu for semantic segmentation, analyzing three distinct datasets of seasonal imagery, with image counts of 1470, 13500, and 940. Among the two, Tiramisu achieved an accuracy of 51%, 37% and 33% on dataset 1 ,2 and 3 respectively , demonstrating its performance in classifying the identified classes effectively, whereas Deeplabv3+ achieved 31%,26% and 25% for dataset 1 ,2 and dataset – 3.

## 1. Introduction

Remote Sensing is the process of acquiring information about objects or regions from a distance, typically using sensors mounted on aircraft or satellites [15]. Satellite imagery refers to images of Earth's surface captured by satellites operated by various governmental and commercial organizations worldwide [11]. With growing concerns over the environmental impact of human activities, monitoring global land use and land cover (LULC) changes has become increasingly important [5]. LULC classification is essential for tracking natural resource distribution and changes across diverse geographical areas [10]. For decades, remote sensing has been a vital tool in generating LULC maps, organizing satellite imagery into distinct categories based on known land use and cover types [11]. Accurate LULC mapping is critical for effective urban planning, agricultural management, and resource conservation [13]. To improve classification accuracy, artificial intelligence (AI) techniques such as neural networks, K-means clustering, Random Forests, and Support Vector Machines (SVM) are widely applied [3]. These advanced methods utilize pattern recognition and computer vision to analyze remote sensing data with high precision [7]. LULC classification plays a crucial role in identifying dominant land use patterns, including agricultural activities, urban development, and natural features such as forests, water bodies, and mangroves [16]. Among various techniques, remote sensing imagery remains the most widely used for capturing LULC data

[8]. Image classification, a fundamental aspect of remote sensing, enables detailed analysis and pattern recognition, supporting accurate mapping and monitoring efforts [4]. It involves applying decision rules that categorize pixels into groups based on their spectral and informational characteristics [10]. Remote sensing, as both a science and an art, involves acquiring and interpreting data about objects or areas without direct physical contact using specialized sensors [15]. LULC classification through remote sensing imagery has been extensively applied in environmental monitoring, change detection surveys [5], urbanization impact assessments [16], and disaster mitigation efforts [17]. Since the introduction of Deep Learning by Hinton et al. in 2006 [8], deep neural networks have significantly advanced in image and video processing, making them powerful tools for remote sensing applications [7]. Deep learning algorithms have revolutionized image interpretation, leading to extensive research in remote sensing image classification [3]. Semantic segmentation, a technique used for pixel-level image classification, assigns each pixel to a specific category [10]. Deep learning has demonstrated exceptional accuracy in computer vision tasks and has immense potential in automating Earth Observation (EO) data analysis [3]. However, pixel-level segmentation of satellite images presents challenges, primarily due to the difficulty of collecting ground truth datasets required for training [13]. This study evaluates the effectiveness of two deep learning models, DeepLabv3+ and Tiramisu, for LULC classification. Tiramisu is a polyhedral compiler designed for both dense and sparse deep learning applications, offering a range of loop optimizations and data structuring techniques [7]. DeepLabv3+, on the other hand, is an advanced semantic segmentation model featuring encoder-decoder architecture for precise image analysis [4]. Both models were applied to three datasets of IRS LISS-III multispectral satellite imagery collected during different seasons in the South Gujarat region, India [8]. The research identified four primary LULC classes: Water Bodies, Vegetation, Uncultivated Land, and Residential Areas [10]. By leveraging deep learning for semantic segmentation, this study demonstrates the potential of advanced AI techniques in automating LULC classification, contributing valuable insights for environmental monitoring and sustainable land management [16].

## 2. Literature review

Dynamic land use and land cover (LULC) changes, along with associated land expropriations, have significantly impacted peri-urban farmers in the rapidly expanding city of Addis Ababa, Ethiopia [2]. Projected LULC maps for 2022 indicate a high level of accuracy, with an overall Kappa value of 0.83 and a correctness percentage of 88.8% [12]. Remote sensing (RS) images were processed using specialized GIS software, ArcGIS 10.8, where false-color composites were generated, and a supervised classification approach employing the maximum likelihood method was applied to produce an accurate LULC map [24].Deep learning models have been increasingly utilized for LULC classification. A study employing deep neural networks demonstrated that the U-Net model achieved an accuracy of 84%, while DeepLabv3+ and Tiramisu attained 29% and 33% accuracy, respectively [6]. Another proposed approach demonstrated high performance, achieving an accuracy of 89.3% and an F-score of 0.820, indicating strong consistency and reliability [1]. Additionally, research suggests that semantic segmentation techniques using deep learning, particularly DeepLabV3+, outperform U-Net in both speed and accuracy [9]. However, despite its high classification accuracy, DeepLabV3+ presents challenges such as a large number of model parameters and inefficient partitioning [14].

# 3. Materials and Methods

## 3.1 Research methodology

Figure 1 illustrates the research methodology for Land Use/Land Cover classification using an IRS LISS-III multispectral image. The methodology consists of several crucial steps:

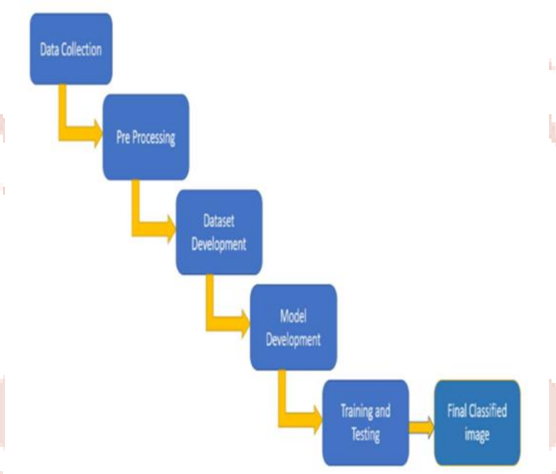


Figure 1. Research Methodology

The methodology for land use and land cover analysis through remote sensing follows a systematic approach. It begins with data acquisition, where the necessary satellite imagery is collected for analysis. Next, image pre-processing is performed to refine and enhance the gathered images by applying essential corrections and transformations. Once the images are processed, dataset compilation involves structuring and annotating the data to create an organized dataset suitable for model training. In the model development and training phase, a classification model is built and trained to recognize patterns in various land cover categories and make accurate predictions. Following this, performance evaluation is conducted to assess the model's effectiveness by measuring its accuracy in classifying different land cover types. Finally, generation of classified imagery results in a visually segmented image that distinctly represents the different land use and land cover classifications. This structured methodology ensures a comprehensive and efficient approach to analyzing land use and land cover using remote sensing technology.

### 3.2 Data acquisition

This research was conducted in the South Gujarat Region, Gujarat State, India, utilizing multispectral remote sensing images from the IRS LISS-III sensor. The LISS-III sensor captures imagery with fewer than 10 bands and provides detailed spectral data with a wavelength resolution exceeding 100 nm. For data collection, 30m × 30m quadrats were systematically placed across the study area, aligning with the spatial resolution of the satellite sensor. The images were stored in separate .tiff files across four spectral bands: Band 2 (Blue), Band 3 (Green), Band 4 (Red), and Band 5 (Near Infrared), each with a spatial resolution of 30 meters. The remote sensing data was obtained from the Indian Space Research Organization (ISRO) via the Bhuvan portal (https://bhuvan-app3.nrsc.gov.in).In addition to satellite imagery, field studies were conducted to document various environmental landscapes and their corresponding land use and land cover (LULC) categories. Ground Control Points (GCPs), with verified latitude and longitude coordinates, were collected for each LULC class using a Garmin eTrex 30 GPS device, ensuring geospatial precision with a positional accuracy of ±4 meters. The selection and placement of GCPs were based on the spatial distribution of the identified land use categories within the study area. Four distinct LULC classes were identified in this study: Water Bodies, Vegetation, Uncultivated Land, and Residential Areas. A comprehensive field survey was conducted to analyze ecological features and land use distribution patterns. The number of sampling points assigned to each class was determined based on their spatial extent within the study region. To enhance classification accuracy, the strategic placement of sampling points was carefully aligned with the identified land use patterns. By integrating high-resolution satellite imagery with ground truth validation, this study ensured precise geospatial referencing and reliable LULC classification.

### 3.3 Pre-Processing

The Indian Remote Sensing (IRS) LISS-III multispectral images consist of four spectral bands, which are combined to generate False Colour Composite (FCC) images for enhanced visual analysis. These FCC images are created by merging multiband .TIFF files, typically using Band 4 (Red), Band 3 (Green), and Band 2 (Blue) to improve feature distinction. To develop a robust dataset for model training, ground truth masks are generated following the FCC image creation. These masks are produced using the maximum likelihood (ML) algorithm, applied to specific regions of interest (ROI) for accurate classification of land cover types. Figure 2 showcases an

FCC image, demonstrating how the combination of spectral bands enhances visualization, while Figure II displays the corresponding ground truth mask, which is used as labeled data for supervised learning. The dataset utilized in this study includes FCC images from multiple seasons, paired with accurately labeled ground truth masks to ensure diversity and reliability in classification. To maintain uniformity, both FCC images and their corresponding masks were resized to 1024 × 1024 pixels, ensuring consistency across all training samples for effective segmentation and classification.

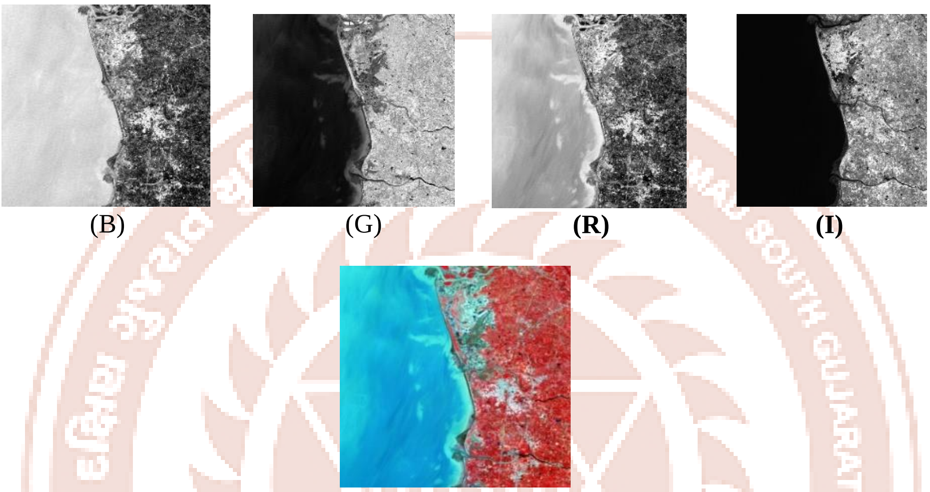


False color composite (FCC) Image

Figure 2. Creation of FCC

The pre-processing steps for land cover classification involve several key stages to ensure optimal data preparation. First, False-Color Composite (FCC) images are created by stacking multiband TIFF images, specifically combining Band 4 (Red), Band 3 (Green), and Band 2 (Blue) to enhance visual interpretation. Figure 1 illustrates the resulting FCC image. Next, ground truth masks are generated to serve as labeled data for model training. These masks are produced using the maximum likelihood (ML) algorithm, applied to small regions of interest (ROI) that correspond to each land cover class. To maintain consistency, both the FCC images and their ground truth masks are resized to 1024 × 1024 pixels. Further, these resized images and masks are divided into smaller patches of 256 × 256 pixels and 128 × 128 pixels, with strides of 128 and 64 pixels, respectively, to enhance model training efficiency. Finally, the processed images and masks are split into two subsets—one designated for training and the other for validation. Figure 2 displays the FCC image, while Figure 3 presents the corresponding ground truth masks, illustrating the structured dataset used for deep learning-based land cover classification.

### 3.4 Creation of Mask

The Maximum Likelihood (ML) classifier was applied to the LISS-III multispectral image data to categorize each pixel into its respective land cover class based on statistical probability. In this method, a pixel is assigned to a class by evaluating the likelihood that it belongs to a particular category, considering the class's statistical characteristics. The mean vector and covariance metrics, derived from the training data, play a crucial role in improving classification accuracy. To support the model training process, ground truth masks were generated using the ML algorithm, which was applied to regions of interest (ROI) for each land cover class. These masks, created after the generation of False-Color Composite (FCC) images, provided labeled training data essential for accurate classification. Figure 3 illustrates the fundamental concepts of the maximum likelihood classification process, highlighting how probabilistic analysis enhances land cover mapping.

Following is a Discriminant Functions Calculated for Each Pixel:

$$\boldsymbol{g_i(x) - \ln p(\omega_i) - 1/2\ln|\Sigma_i| - 1/2(x - m_i)^t \Sigma_i^{-1}(x - m_i)} \qquad (1)$$

Where i is class, x is n-dimensional data in which n represents the total number of bands. p(ωi) represents the chance that class ωi occurs in the image, |Σi| is the determinant of the covariance matrix, Σi-1 is an inverse matrix the mean vector represents by mi.

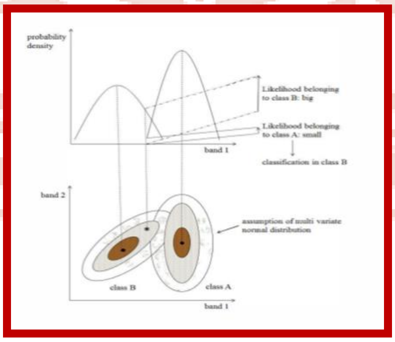


Figure 3 : Basic concept of ML

After creating FCCs for each image, ground truth masks were created that will be used to train a model. These masks are created using the maximum likelihood algorithm on a small region of interest for each class. Figure 4 shows the ground truth masks.

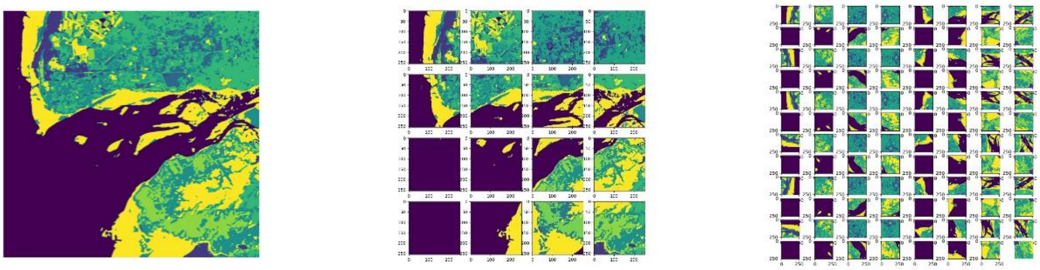

Figure 4: Ground Truth Mask

The FCC images and their corresponding masks are resized to 1024 x 1024 pixels and then divided into patches of 256 x 256 pixels with a stride of 128 pixels.

### 3.5 Methodology

This study evaluated the performance of two advanced segmentation models, DeepLabv3+ and Tiramisu, for land use and land cover (LULC) classification using IRS LISS-III multispectral satellite images. Semantic segmentation was employed to assign class labels at the pixel level, categorizing the landscape into four distinct classes: Water Bodies, Vegetation, Uncultivated Land, and Residential Areas. DeepLabv3+, developed by Google and open-sourced in 2016, enhances its predecessor, DeepLabv3, by incorporating a decoder module that improves segmentation accuracy, particularly along object boundaries. The model operates in two primary stages: encoding and decoding. In the encoding phase, essential image features are extracted using a convolutional neural network (CNN), where Aligned Xception replaces ResNet-101, eliminating max-pooling operations in favor of depth-wise separable convolutions to enhance computational efficiency. In the decoding phase, extracted features are upsampled through a structured approach that first applies a 4× upsampling, concatenates low-level encoder features, processes them with 1×1 convolutions to reduce channel dimensions, and then refines them through 3×3 convolutions before a final 4× upsampling restores the image to its original resolution. This structured upsampling strategy significantly improves segmentation precision, particularly along object edges, enabling more detailed and accurate classification. The DeepLabv3+ model architecture, illustrated in Figure 5, highlights its encoder-decoder structure, demonstrating its effectiveness in refining LULC classification results.

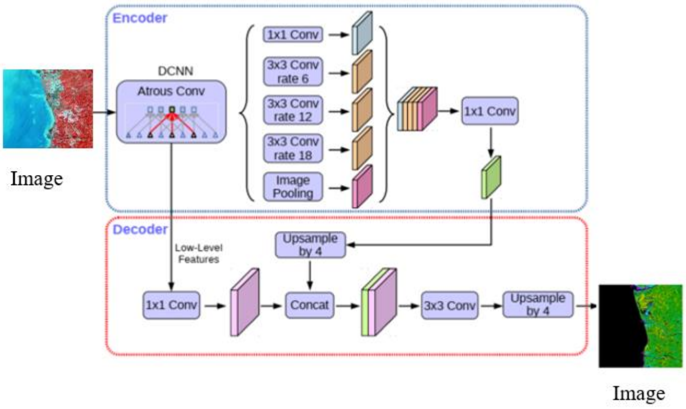


Figure 5: Deeplabv3+ model. [ref: https://arxiv.org/ab s/1802.02611]

The Tiramisu framework is an advanced deep learning compiler designed to optimize both dense and sparse neural networks while supporting data-parallel algorithms. It performs a wide range of loop transformations and memory optimizations, enhancing computational efficiency. Unlike conventional compilers, Tiramisu is the only open-source deep learning compiler that effectively optimizes sparse neural networks and facilitates distributed computing architectures. It employs dependence analysis to ensure the correctness of complex loop modifications, making it highly effective for high-performance computations. The framework has demonstrated strong capabilities in deep learning tasks, including convolutional operations, activation functions (ReLU), pooling mechanisms, and matrix computations. Built on an enhanced U-Net architecture, the Tiramisu model is considerably larger and requires longer training times compared to other models. However, its powerful optimization techniques enable it to excel in semantic segmentation tasks, making it a valuable tool for land use and land cover classification. Figure 6 illustrates the Tiramisu model architecture.

$$xl = Hl\ (xl - 1) \tag{4}$$

in standard convolution, xl is computed by applying a non-linear transformation Hl to the output of the previous layer xl-1.

$$xl = Hl\ (xl - 1) + xl - 1 \tag{5}$$

ResNet introduces a residual block that sums the identity mapping of the input to the output of a layer

.

$$xl = Hl\ ([\ xl\ -1,\ xl\ -2,\ \ldots\ldots\ldots.,\ X0]) \tag{6}$$

DenseNet input concatenates all previous feature outputs in a feed forward fashion for convolution.

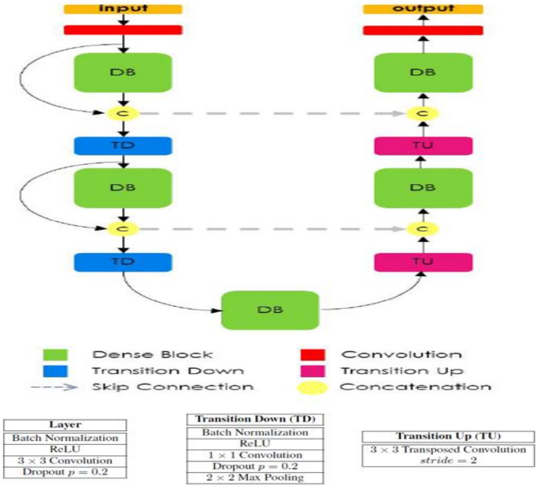


Figure 6: Tiramisu Architecture [Ref https://towardsdatascience.com/review-fc-densenet-one-hundred-layer-tiramisu-semantic-segmentation-22ee3be434d5]

### 3.6 Algorithm Steps

The image segmentation and classification process consists of several key stages. In the pre-processing phase, input images are adjusted by aligning them with spatial reference points and applying masks to isolate relevant regions, utilizing Bands 2–4 of IRS LISS-III imagery. Next, in the class selection stage, land cover categories such as Water Bodies, Vegetation, Uncultivated Land, and Residential Areas are defined, with the ENVI ROI Tool used to delineate these classes within the study area. The model building and training phase involves designing a deep learning model, configuring hyperparameters such as learning rates and epochs, and training the model using pre-processed images with assigned land cover classes. Once trained, the model is saved for future applications. In the model application phase, the trained model is deployed to classify pixels in target images, generating a segmented output that visually represents different land cover types. Finally, in the outcome verification stage, the classification results are validated to ensure accuracy in representing the spatial distribution of land cover classes. This structured workflow integrates data preparation, model training, classification, and verification, ensuring a systematic approach to land use and land cover analysis.

### 3.7 Training Configuration

During the data preprocessing stage, input images were normalized by restricting pixel values to the range [0.0, 255.0], ensuring uniformity across all samples. To accurately encode land cover classes, a one-hot encoding method was applied to the segmentation masks. To further enhance model generalization and improve dataset variability, data augmentation techniques such as rotations, flips, and translations were applied to both images and masks. These transformations introduced realistic variations, reducing the risk of overfitting and enabling the model to learn robust feature representations. A custom data pipeline was designed to preprocess and seamlessly feed augmented images and masks into the model in a structured format suitable for training. This ensured that augmentation and encoding steps were consistently applied throughout the process. Additionally, Table 1 outlines the hyperparameters and training configurations, including learning rates, batch sizes, and network parameters, providing essential insights for reproducibility and further optimization of the model's performance.

**Table 1.** Training configuration

| Hyperparameters & Configurations | Values |
|---|---|
| Train Batch Size | 16 |
| Validation Batch Size | 16 |
| Input Image Shape | (256, 256, 3), (128,128,3) |
| Number of classes | 4 |
| Epochs | 50 |
| Loss Categorical | Focal Loss* |
| Optimizer | Adam |
| Metrics | Dice Coefficient* |
| Class Weights | [1.69941, 0.53043, 1.23977, 1.38949] |

## 4. Result and discussion

The experimental setup for this study involves multiple key components. Windows 11 served as the operating system for data processing and model training. ENVI 4.7 software was utilized for preprocessing tasks such as image masking and extracting training samples essential for model training. The classification model was implemented using Python and OpenCV, leveraging the DeepLabv3+ architecture with the Adam optimizer for land cover classification. Despite its advanced capabilities, the model attained a relatively low accuracy of 31% on the dataset. To analyze model performance, Figures 7, 9, and 11 present the training logs, illustrating key performance metrics during the training process. Furthermore, Figures 8, 10, and 12 showcase the classification results, providing a detailed quantitative assessment of each identified land cover category along with its spatial distribution. This experimental framework offers valuable insights into model effectiveness and highlights potential areas for refinement in future studies.

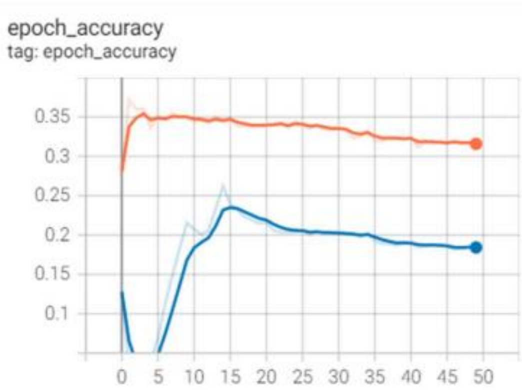


Figure 7: training log for Deeplabv3+ on dataset -1

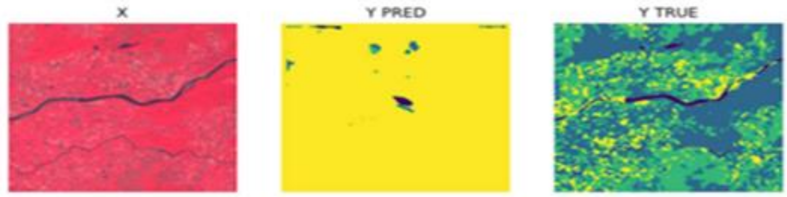


{0: 1.9480705261230469}
{0: 1.9480705261230469, 1: 15.830612182617188}
{0: 1.9480705261230469, 1: 15.830612182617188, 2: 1.4016151428222656}
{0: 1.9480705261230469, 1: 15.830612182617188, 2: 1.4016151428222656, 3: 80.8197021484375}

Figure 8: Result predicted by the model on dataset -1

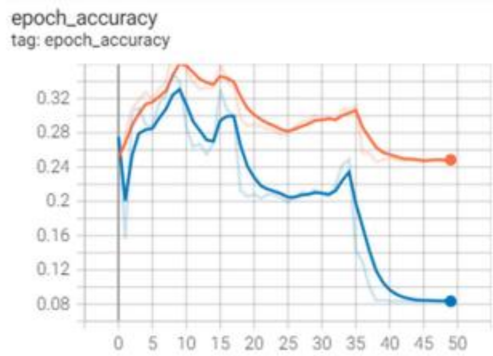


Figure 9: training log for Deeplabv3+ on dataset -2


{0: 10.333633422851562}
{0: 10.333633422851562, 1: 4.3750762939453125}
{0: 10.333633422851562, 1: 4.3750762939453125, 2: 60.938262939453125}
{0: 10.333633422851562, 1: 4.3750762939453125, 2: 60.938262939453125, 3: 24.35302734375}

Figure 10: Result predicted by the model on dataset -2

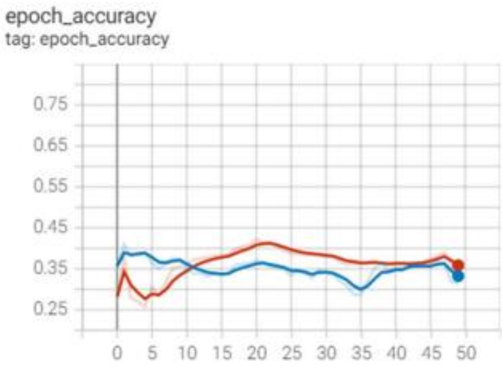


Figure 11: training log for Deeplabv3+ on dataset -3

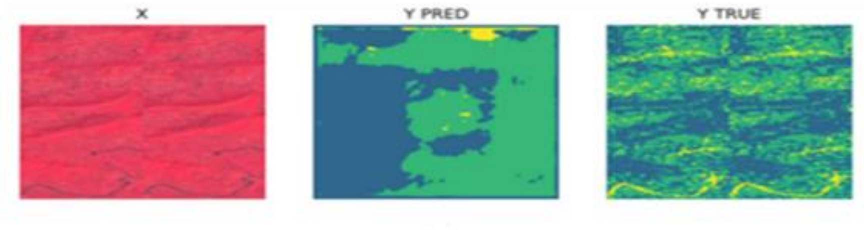


```
{0: 0.079345703125}
{0: 0.079345703125, 1: 54.05893325805664}
{0: 0.079345703125, 1: 54.05893325805664, 2: 44.4244384765625}
{0: 0.079345703125, 1: 54.05893325805664, 2: 44.4244384765625, 3: 1.4372825622558594}
```

Figure 12: Result predicted by the model on dataset -3

Figures 13 and 15 present the results of land use and land cover (LULC) classification performed by the Tiramisu model on Dataset 1. The model was trained using the Adam optimizer and achieved an accuracy of 51%. The predicted classification output is illustrated in Figures 14, 16, and 17, where each pixel in the image is assigned to a specific land cover class as identified by the model. Additionally, class-wise quantification outlines the distribution and proportion of each identified land cover category within the resulting image, offering insights into the relative coverage of different land use types across the study area.This output highlights the model's capability to accurately classify various land cover types while also revealing areas for potential improvement in accuracy. Figure 10(b) provides further visual representation of the classification results. These findings demonstrate the Tiramisu model's effectiveness in processing remote sensing imagery and generating detailed LULC maps, though refinements may further enhance its performance.

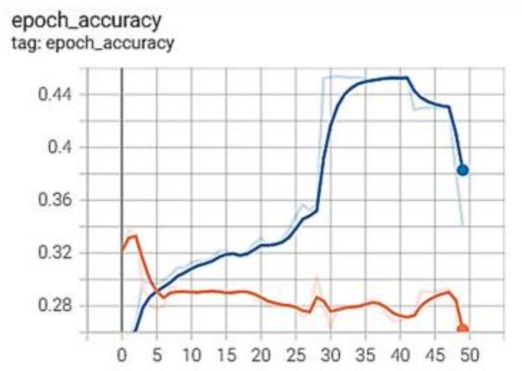


Figure 13: training log for Tiramisu

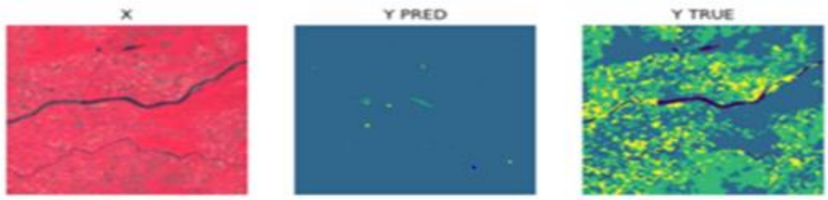


```
{0: 0.09031295776367188}
{0: 0.09031295776367188, 1: 98.95648956298828}
{0: 0.09031295776367188, 1: 98.95648956298828, 2: 0.4422187805175781}
{0: 0.09031295776367188, 1: 98.95648956298828, 2: 0.4422187805175781, 3: 0.5109786987304688}
```

Figure 14: Result predicted by the model

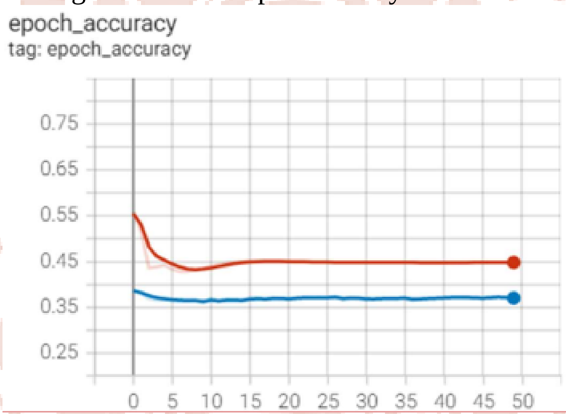


Figure 15: training log for Tiramisu

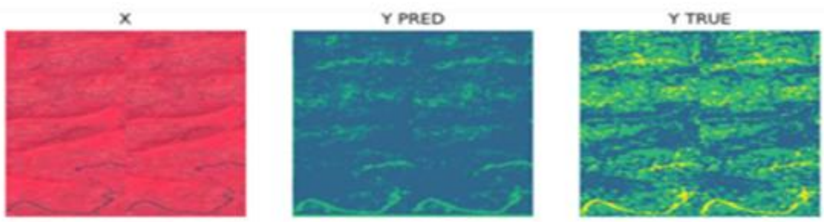


```
{0: 0.1911163330078125}
{0: 0.1911163330078125, 1: 92.5893783569336}
{0: 0.1911163330078125, 1: 92.5893783569336, 2: 7.2170257568359375}
{0: 0.1911163330078125, 1: 92.5893783569336, 2: 7.2170257568359375, 3: 0.00247955322265625
```

Figure 16: Result predicted by the model

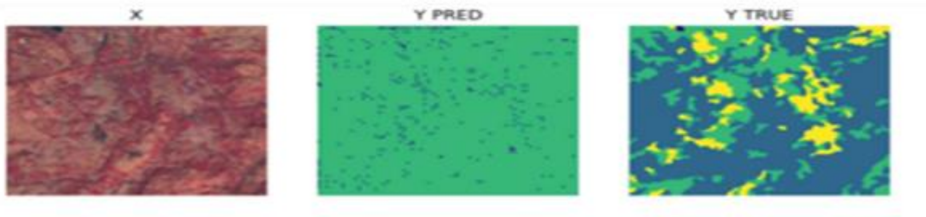


```
{0: 1.639556884765625}
{0: 1.639556884765625, 1: 0.0682830810546875}
{0: 1.639556884765625, 1: 0.0682830810546875, 2: 98.2921600341 7969}
```

Figure 16: Result predicted by the model

Table 2 presents the accuracy comparison of various classification models evaluated in this study. The results clearly indicate that the Tiramisu model outperforms DeepLabv3+ in terms of classification accuracy. While DeepLabv3+ achieved a relatively low accuracy of 31% on dataset-1, 26% on dataset-2 and 25% on dataset -3 , Tiramisu attained a moderate accuracy of 51% on dataset-1,37% on dataset-2 and 33% on dataset -3, demonstrating its superior performance in identifying land use and land cover (LULC) types. This comparison underscores Tiramisu's effectiveness for LULC classification, though both models exhibit scope for further improvement. The findings suggest that Tiramisu is a more suitable choice for this classification task, offering better precision and reliability than DeepLabv3+ in this specific application.

Table 2 : Model Accuracy

| | | | | |
|---|---|---|---|---|
| Deeplabv3+ | Adam | 50 | Dataset - 1 | 31 |
| Deeplabv3+ | Adam | 50 | Dataset – 2 | 26 |
| Deeplabv3+ | Adam | 50 | Dataset - 3 | 25 |
| Tiramisu | Adam | 50 | Dataset - 1 | 51 |
| Tiramisu | Adam | 50 | Dataset – 2 | 37 |
| Tiramisu | Adam | 50 | Dataset - 3 | 33 |

## 5. Conclusion

The application of intelligent systems, particularly deep learning, has proven to be highly effective for Land Use Land Cover (LULC) classification, offering notable advantages over traditional approaches. These advanced systems provide a cost-efficient and time-saving alternative compared to conventional visual interpretation or standard machine learning techniques. This study, conducted in the South Gujarat region of India, analyzed data collected across multiple seasons (October, January, and May) to assess the performance of deep learning models in LULC classification. The research utilized the Deeplabv3+ and Tiramisu deep learning architectures, both of which were trained and tested on LISS-III multispectral satellite imagery. The study successfully classified four primary LULC categories: water bodies, barren land, residential zones, and vegetative regions. Among the models evaluated, Tiramisu demonstrated superior accuracy, achieving 51% on dataset-1, 37% on dataset-2, and 33% on dataset-3, whereas Deeplabv3+ attained 31% accuracy on dataset-1, 26% on dataset-2, and 25% on dataset-3. These findings emphasize the effectiveness of deep learning in automating LULC classification and highlight the Tiramisu model's superior performance for this application. This paper underscores the increasing importance of deep learning in remote sensing, offering a reliable and efficient approach for land cover analysis. By leveraging LISS-III multispectral imagery, the models effectively processed and categorized land use data, providing valuable insights for environmental monitoring and sustainable land management.

**Conflict of interest statement:** On behalf of all authors, the corresponding author states that there is no conflict of interest.

**Competing Interests:** Not Applicable

**Funding Information:** No funding was received. This research was conducted without external funding

Author contribution

**Nirav Desai:** Principal author

Conceptualization, methodology, data analysis, specific analyses and writing of the original draft

**Akruti Naik:** Second Author

Data collection, literature review, methodology, data analysis, specific analyses, and their relevant tasks

**Data Availability Statement:** The data that support the findings of this study are available from website https://bhuvan-app3.nrsc.gov.in, provided by the Indian Space Research Organization (ISRO)

**Research Involving Human and /or Animals:** Not Applicable

**Informed Consent:** Authors in this study provided informed consent, acknowledging their understanding of the research's purpose, procedures, and potential risks

## 6. References

[1] Al-Taei, A. I., Alesheikh, A. A., & Darvishi Boloorani, A. (2023). Land use/land cover change analysis using multi-temporal remote sensing data: A case study of Tigris and Euphrates Rivers Basin. *Land*, *12*(5), 1101.

[2] Ayenachew, Y. A., & Abebe, B. G. (2024). The dynamics of urbanization, land use land cover changes, and land expropriation in Addis Ababa, Ethiopia. *Frontiers in Environmental Science*, *12*, 1439954.

[3] C. D. Storie and C. J. Henry, “Deep learning neural networks for land use land cover mapping,” IGARSS 2018 - 2018 IEEE International Geoscience and Remote Sensing Symposium, pp. 3445–3448, 07 2018.

[4] Campbell, J. B., & Wynne, R. H. (2008). Introduction to Remote sensing 4th Edition

[5] Chen,Y.-C.,Chiu, H.-W., Su,Y.-F.,Wu, Y.-C., andCheng,K.-S. (2017). Does urbanization increase diurnal land surface temperature variation? Evidence and implications. Landscape Urban Plann. 157, 247–258. doi:10.1016/j.landurbplan.2016.06.014

[6] [25] Desai, N., & Shukla, P. (2023). Performance of deep learning in land use land cover classification of indian remote sensing (IRS) LISS-III multispectral data. *International Journal on Recent and Innovation Trends in Computing and Communication*, *11*(3), 128-134.

[7] Dian-lai, W., Ai-xia, S., & Wen-ping, L. (2020, November). Application of deep neural networks in classification of medium resolution remote sensing image. In Journal of Physics: Conference Series (Vol. 1682, No. 1, p. 012014). IOP Publishing.

[8] Hinton, G. E., Osindero, S., & Teh, Y. W. (2006). A fast learning algorithm for deep belief nets. Neural computation, 18(7), 1527-1554.

[9] [27] Herlawati, R. T. H. (2024). Land Cover Segmentation of Multispectral Images Using U-Net and DeeplabV3+ Architecture. *Jurnal Ilmu Komputer dan Informasi (Journal of Computer Science and Information)*, *17*(1).

[10] Homer, C., Huang, C., Yang, L., Wylie, B., & Coan, M. (2004). Development of a 2001 national land-cover database for the United States. Photogrammetric Engineering & Remote Sensing, 70(7), 829-840.

[11] J. P. D. Chan, "Evaluation of Random Forest and Adaboost treebased ensemble classification and spectral band selection for ecotope mapping using airborne hyperspectral imagery.," Remote Sensing of Environment, vol. 112, p. 2999–3011, 2008.

[12] Ketema, D., & Bekele, A. (2024). Modeling the Land use Land cover changes and its impacts on agricultural land area by using GIS and RS at Fitche town, Central Ethiopia.

[13] Lu, D., & Weng, Q. (2007). A survey of image classification methods and techniques for improving classification performance. International journal of Remote sensing, 28(5), 823-870.

[14] Lu, J., Zhou, B., Wang, B., & Zhao, Q. (2022, December). Land cover classification of remote sensing images based on improved Deeplabv3+ Network. In *Journal of Physics: Conference Series* (Vol. 2400, No. 1, p. 012035). IOP Publishing.

[15] Sarah C. Goslee" Analyzing Remote Sensing Data in R: The Landsat Package", Journal of Statistical Software, July 20i I, Volume 43, Issue http://www.jstatsoft.orgl

[24] Sati, V. P., Banerjee, S., & Roy, C. LAND USE AND LAND COVER DYNAMICS AND FACTORS AFFECTING IT IN THE CENTRAL HIMALAYA.

[16] Suneetha, Manne, et al. "Object based Classification of Multispectral Remote Sensing Images for Forestry Applications." Proceedings of the 2020 3rd International Conference on Image and Graphics Processing. 2020.

[17] Xu, X., Chen, Y., Zhang, J., Chen, Y., Anandhan, P., & Manickam, A. (2021). A novel approach for scene classification from remote sensing images using deep learning methods. European Journal of Remote Sensing, 54(sup2), 383-395.

[18] https://arxiv.org/ab s/1802.02611

[19] https://towardsdatascience.com/review-fc-densenet-one-hundred-layer-tiramisu-semantic-segmentation-22ee3be434d5